CdSe/CdS/ZnS nanocrystals decorated with Fe₃O₄ nanoparticles for point-of-care optomagnetic detection of cancer biomarker in serum

Anjum Qureshi, Ali Tufani, Gulcan Corapcioglu, Javed H. Niazi*

Sabanci University Nanotechnology Research and Application Center (SUNUM), Istanbul, 34956, Turkey

ABSTRACT

Early diagnosis of a progressive cancer disease is currently limited due to lack of adequate point-of-care (PoC) diagnostic tools. PoC diagnosis enables detecting early signs of a disease and pave way to disease prevention. Here, we developed an immuno-optomagnetic quantum dots based PoC assay for early detection of a cancer biomarker, human epidermal growth factor receptor-2 (hErbB2) protein in serum. This assay utilizes immuno-optomagnetic quantum dots (MQDs-Ab2) nanoarchitectures with unique orientation comprised of core CdSe/CdS/ZnS QD nanocrystals surrounded by layers of magnetic Fe₃O₄ nanoparticles (MNPs) and a bioactivated borofloat PoC-chip (Ab1). The MQDs-Ab2 and the PoC-chips were designed to bind same hErbB2 analyte, but both bind with distinct epitopes. First, free hErbB2 protein from serum was captured by MQDs-Ab2 forming immuno-optomagnetic MQDs-Ab2-hErbB2 complex, which was isolated and presented to bioactivated PoC-chips. The immuno-optomagnetic signal from chips was directly visualized by naked-eye after exposing chips with a UV-torch and the signal was directly measured within 30 min by computing RGB intensities using a smartphone camera and a colorimeter-app. The immuno-optomagnetic QDs based PoC-chip exhibited the detection range of 620 pg mL⁻¹ ~5 ng mL⁻¹ hErbB2 protein in serum. The MQDs-Ab2 rendered biospecificty, magnetic and optical functionality to PoC detection and provided advantages of speed, sensitivity, portability and low-cost, which is most desired in resource limited settings. The developed PoC chip assay provided an accurate quantitative cancer biomarker detection with high sensitivity and specificity that required no laboratory equipment and is also potentially applicable to the detection of many other biomarkers.

1. Introduction

One of the major problems in diagnosis or preventing a progressive cancer disease is the lack of a rapid, sensitive and less-expensive point-of-care (PoC) diagnostic tool. Development of such PoC diagnostic tools could enable detecting early warning signs, which pave way to prevent progression of the disease. Breast cancer in women is regarded as the second leading cause of cancer related mortality worldwide ((WHO), 2018). It is estimated that 2.09 million breast cancer related cases reported causing 627,000 deaths worldwide according to a [1]) report. These figures account for about 15 % of all cancer deaths among women ((WHO), 2018). A number of conventional and well-established diagnostic methods are being currently used, such as mammogram, tissue biopsy, CT, MRI, CAT or PET scans [2,3], genetic screening for BRCA1 gene mutations [4], fluorescence in-situ hybridization (FISH) [5–7], enzyme-linked immunosorbent (ELISA) [8,9] radioimmunoassay [10] and chemiluminescence immunoassays [6,11,12]. All the above techniques are not easily accessible nor suitable for PoC settings apart

from being highly expensive, require long testing times, demand sophisticated instruments and required professionally trained personnel to perform tests. Therefore, essential repetitive testing for cancer diagnosis or its monitoring by the existing approaches makes it extremely difficult to clinicians or cancer patients.

Most sensitive diagnostic approaches that are available, such as FISH and ELISA require laborious washing steps in order to separate unbound analyte and labeling free ligands/receptors to minimize the non-specific fluorescent background signal and complex matrix susceptibility. These parameters affect the stability and structure of target probe biomolecule or specificity and weaken the sensitivity of immunoassay platform. Despite of the existing diagnostic methods have been practiced for over a decade. Yet, none of the existing methods found promising for early cancer diagnosis. Therefore, it is imperative to develop novel diagnostic methods that are affordable, rapid and sensitive in PoC settings, which paves way to early diagnosis, prevention or monitoring the progression of cancer.

Extension of traditional diagnostic approaches into lab-on-achip and

PoC diagnostics currently presents significant challenges, especially when affordability, speed and accuracy of diagnosis are critically important. PoC based diagnosis offer advantageous of speed, sensitivity, specificity and compatibility of using them near the patient bedside. Blood serum is a preferred source of the sample especially for performing PoC based cancer diagnosis which is simple and easy to obtain. The key factors that indicate the disease are biomarkers in serum and their levels. Presence of a specific serum biomarker associated with a cancer disease and its levels in detectable amounts enables accurate prediction or progression of cancer. One such promising biomarker is human epidermal growth factor receptor 2 (hErbB2 or Her2) protein, which is associated with multiple cancer types, but mainly breast cancer. Extracellular domain (ECD) of cleaved hErbB2 protein in the blood stream is associated with a high risk of cancer disease, which can be used as an indicator of increased ErbB2/Her2 expression. The clinical prognostic and predictive usefulness of the serum hErbB2 levels is warranted for clinic-pathologic parameters and therapy monitoring marker [5–7,13]. In relation to other cancer-types, hErbB2 protein has been found overexpressed in ovarian, lung, colorectal, bladder, pancreatic, colon, endometrial and oral cancers [13,14]. It is also found overexpressed by 10–30 % in gastric/gastroesophageal cancers and that hErbB2 protein is regarded as a prognostic and predictive biomarker [13]. Therefore, breast cancer patients' blood samples found to have elevated hErbB2 protein concentrations ($15 - 75$ ng mL^{-1}) compared to those observed in normal individuals with $2 - 15$ ng mL^{-1} [6,8,11]. Early detection and monitoring the serum hErbB2 protein levels can promote the diagnosis speed, screening and enable successful treatment of cancer disease and increase survival rate of cancer patients. Therefore, there is an urgent need for a sensitive, rapid and accurate technology platform for PoC based detection of cancer biomarker in serum, tissue or body fluids.

Chemical combination of QDs and magnetic iron oxide nanoparticles (MNPs) have provided multimodal functionality that has major advances in bio-labeling and MR imaging because of combined optical and magnetic (optomagnetic) properties in a single nanomaterial, which enable simultaneously bio-labeling, imaging, sorting and separation processes [15,16]. Only few reports have been focused on fabrication of magnetic QDs (MQDs) and their utility in PoC platforms. For instance, magnetic QDs have been used for the lateral-flow immunoassay (LFIA) that utilizes larger magnetic nanoparticles (MNPs) over 100 nm surface coated with smaller QDs for the detection of prostate specific antigen (PSA) [17]. However, use of LFIA-like methods rely heavily on migration of nanoparticles in a complex lateral-flow matrix that are prone to impeding the nanoparticles within the matrix and affect the sensitivity. Smaller nano-sized MNPs are required to protect QDs by chemically defining their architecture and orientation, such as QD-nanocrystals being surrounded by MNPs but not vice versa. Such QD-to-MNPs orientation could provide the PoC based system to generate more stable, sensitive and accurate signal for detection of analytes. Other studies utilizing similar MQDs have been reported for detection and separation of cells and biomarkers based on complimentary engineered DNA/RNA sequences [18–21]. QD-nanoprobes utilized in such immunoassays were mainly fabricated by high temperature precursor decomposition, doping, encapsulation of MNPs and QDs using silica or polymer matrix and cross-linking methods. The latter three approaches are limited because of loss of magnetic property due to disordered magnetic crystal structure, interfacial instability of available doped material and NP aggregation and difficulty with sequential synthesis procedures, respectively.

In this study, an immuno-optomagnetic PoC detection assay is designed for detecting and quantifying a model cancer biomarker, hErbB2 protein in human serum. The PoC chip assay is based on multifunctional MQDs-Ab2 and preactivated borofloat chip (Scheme 1a–f). The MQDs-Ab2 were made of unique size-controllable nanoarchitecture and orientation in which core-shell-shell CdSe/CdS/ZnS QD nanocrystals being shielded by surrounding MNPs whose surface was

bioactivated. The magnetic nature of MQDs-Ab2 allowed rapid isolation and concentration of MQDs-Ab2-hErbB2 complex that was charged on Ab1-arrays-on-PoC-chip. Immuno-optomagnetic signal from chip generated was directly visualized with a naked eye by simply flashing with a hand-held UV-torch and the detection was made within 30 min. The signal was also captured using a smartphone equipped with a camera and colorimeter app that computed RGB-signal from chip and provided accurate quantitative measurement of hErbB2 analyte in serum. The immuno-optomagnetic PoC chip assay provided advantages of speed, sensitivity, portability and low-cost that is most desired in PoC diagnostic applications in resource limited settings.

2. Experimental section

2.1. Materials

All materials, proteins, antibodies and reagents used are described in Supplementary Information (SI) section.

2.2. Synthesis of aspartate stabilized magnetic Fe₃O₄ nanoparticles (MNPs)

First, L-aspartic acid capped MNPs ($7 \sim 12$ nm) were synthesized using a modified co-precipitation method previously reported [22] and the details are described in SI section.

2.3. Gradient synthesis of single-color CdSe-CdS-ZnS nanocrystals

In this method, soon after the growth of core nanocrystals, the CdS and ZnS shells were formed in a gradient manner simultaneously. Gradient synthesis of single color green CdSe core nanocrystals with CdS and ZnS shells was performed using previously described methods with slight modification for green nanocrystals [23] and red/orange nanocrystals [24].

For green nanocrystals, first, Se-S solution was prepared in a glovebox by dissolving 0.316 g selenium powder and 0.128 g sulfur powder in 3 mL TOP and placed in a desiccator under vacuum until use. A three-necked flask containing 0.025 g CdO, 0.87 g zinc acetate, 2.75 mL oleic acid and 10 mL octadecene was degassed by heating for 1 h at 150 °C under vacuum. Argon gas was then introduced into the flask from an inlet connected to a condenser, while vacuum tube connected at the outlet, and the reaction temperature was raised to 310 °C. After stabilizing the temperature to 310 °C, 1.5 mL of above Se-S solution was quickly injected to the solution while maintaining the temperature to 304 °C and waited for 20 min for reaction to complete. This procedure was optimized to obtain a single color (green) nanocrystals, while a slightly different method was used for the synthesis of single-color red/orange CdSe/CdS/ZnS nanocrystals and subjected to ligand exchange reaction as described in SI-section.

2.4. Synthesis of magnetic quantum dots (MQDs)

The water-soluble, core-shell-shell CdSe/CdS/ZnS QD nanocrystals (0.28 mg) with free carboxyl functionality were suspended in 0.5 mL deionized water and dispersed by sonication for 5 min using a miniprobe ultrasonicator (Sonopuls mini20) ensuring their homogenous dispersion. To this, 100 μL of freshly prepared 150 mM of 1-ethyl-3-(3-dimethylaminopropyl)carbodiimide hydrochloride (EDC) was added and incubated for 5 min and then added 100 μL of 300 mM *N*-hydroxysuccinimide (NHS). The above reaction mixture was incubated for 5 min and the EDC-activated bright fluorescent nanocrystals were mixed with 1 mL of 10 mg/mL of Asp-MNPs ($7 \sim 12$ nm) suspension. The mixture was incubated for 2 h at room temperature for covalent coupling under vigorous shaking. The resulting reaction mixture contained hybrid CdSe/CdS/ZnS@MNPs nanoparticles (magnetic quantum dots, MQDs) were magnetically separated and resuspending in PBS solution, pH 7.4 in three buffer exchanges. Coating of MNPs on QD nanocrystal
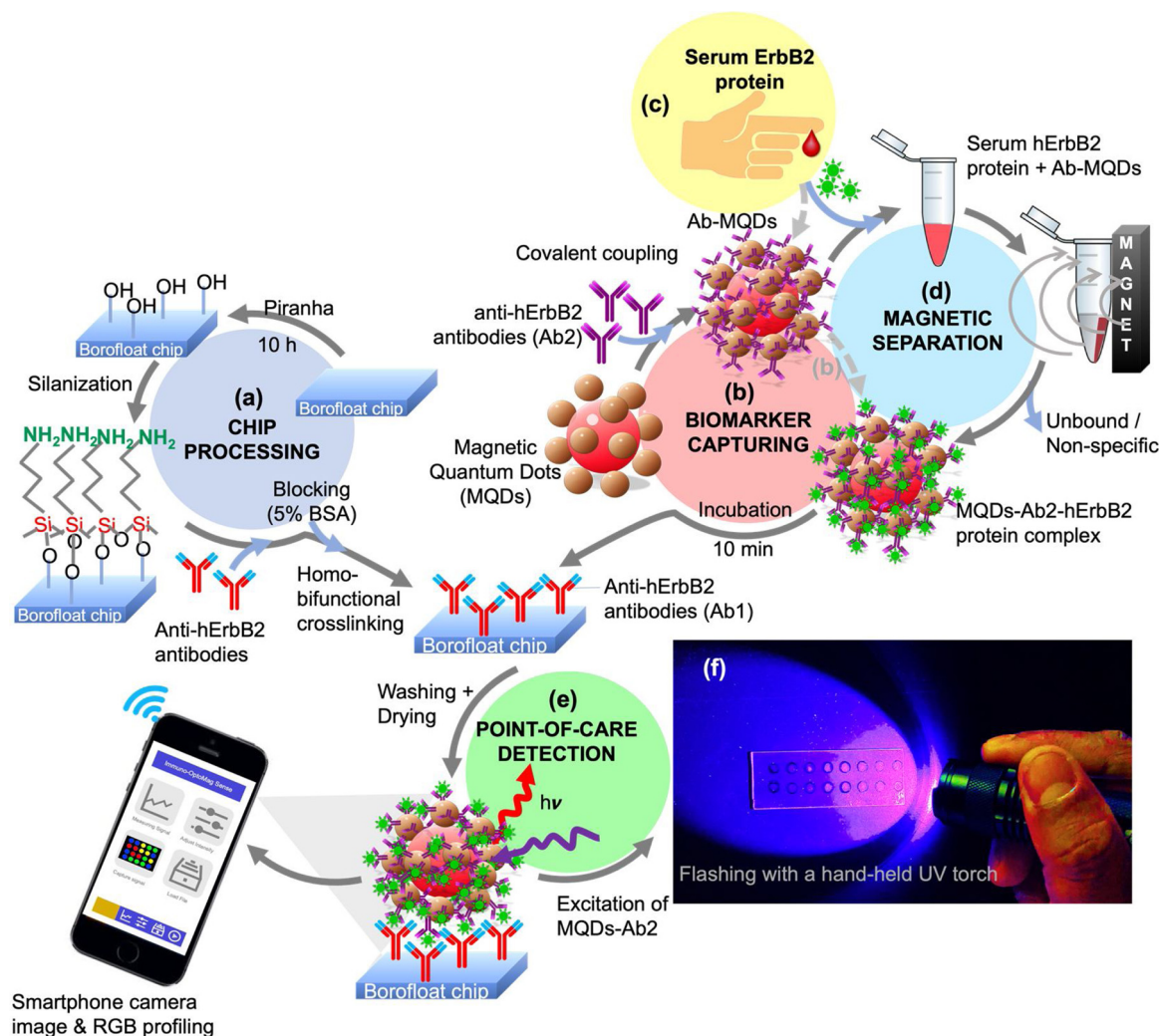
Scheme 1. Schematic illustration of point-of-care immuno-optomagnetic assay for detection of ErbB2/Her2 breast cancer biomarker from a real-serum sample. (a) Functionalization of borofloat chips with anti-hErbB2 antibodies (Ab1). (b) Bioconjugation of optomagnetic MQDs with second anti-hErbB2 antibodies (Ab2). (c-d) Capturing of hErbB2/Her2 protein (cancer biomarker) and magnetic separation of MQDs-Ab2-hErbB2 complex formation. (e) Sandwiching of MQDs-Ab2-hErbB2 complex on to Ab-activated chips to capture hErbB2/Her2 protein present in the sample, and (f) visualization of the diagnostic signal from PoC immuno-opto-magnetic assay chip by a naked eye or using a smartphone camera equipped with RGB profiling algorithm.

surfaces was confirmed after magnetically separated MQDs visibly appeared bright fluorescent in nature upon direct UV irradiation at 365 nm, which accompanied by disappearance of fluorescence from the supernatant solution. In this study, green MQDs showed weak emission intensity as compared with orange MQDs, therefore only orange MQDs were utilized for PoC assays.

2.5. Characterization

All physico-chemical characterizations and methods are described in the SI section.

2.6. Fabrication of chip

Borofloat chips with a dimension of 25 × 73 mm and 1.2 mm thick were purchased from a local supplier. These chips were cleaned using piranha solution (H_2SO_4:H_2O_2 in 5:1 ratio) that rendered hydrophilicity on chip surfaces with hydroxyl groups as well as ensured removal of metals and organic contaminants. Piranha treated chips were then rinsed with deionized water and dried with a nitrogen gun. Clean hydroxyl surfaces of chips were silanized by immersing in a 35 % (3-aminopropyl)triethoxysilane (APTES) solution prepared in acetone

while constant shaking for 4 h. The chips were removed, rinsed thrice with acetone and dried using a nitrogen gun. Silanized chips were then subjected to activation by incubation in 0.05 % glutaraldehyde solution for 1 h and the activated chips were rinsed with deionized water and dried. The activated chip surface was marked using a glass marker with the aid of a clean plastic mask that left imprints of multiple rings in arrays with 5 mm ring diameter, each separated by a 5 mm distance. The inner ring areas were assigned for a series of on-chip antibody immobilization by overnight incubation with 5 μL of 45 μg/mL human ErbB2/Her2 antibodies (Ab1) at 4 °C in a humid chamber. Following this step, the chips were rinsed several times by aspiration with a fresh PBS solution. Free or unoccupied regions on chip were blocked with 5% BSA protein in PBS solution after incubation at 4 °C for 3 h. The chips were rinsed with PBS and dried using a nitrogen gun and stored at 4 °C until use. The immunoreactions can thus be carried out on chips within the assigned ring circumferences, where ErbB2/Her2 specific antibodies were functionalized.

2.7. hErbB2-free serum sample preparation and protein spiking

Normal serum samples free of hErbB2 protein were prepared and spiked with known ErbB2/Her2 protein concentrations, such as 0, 0.62,
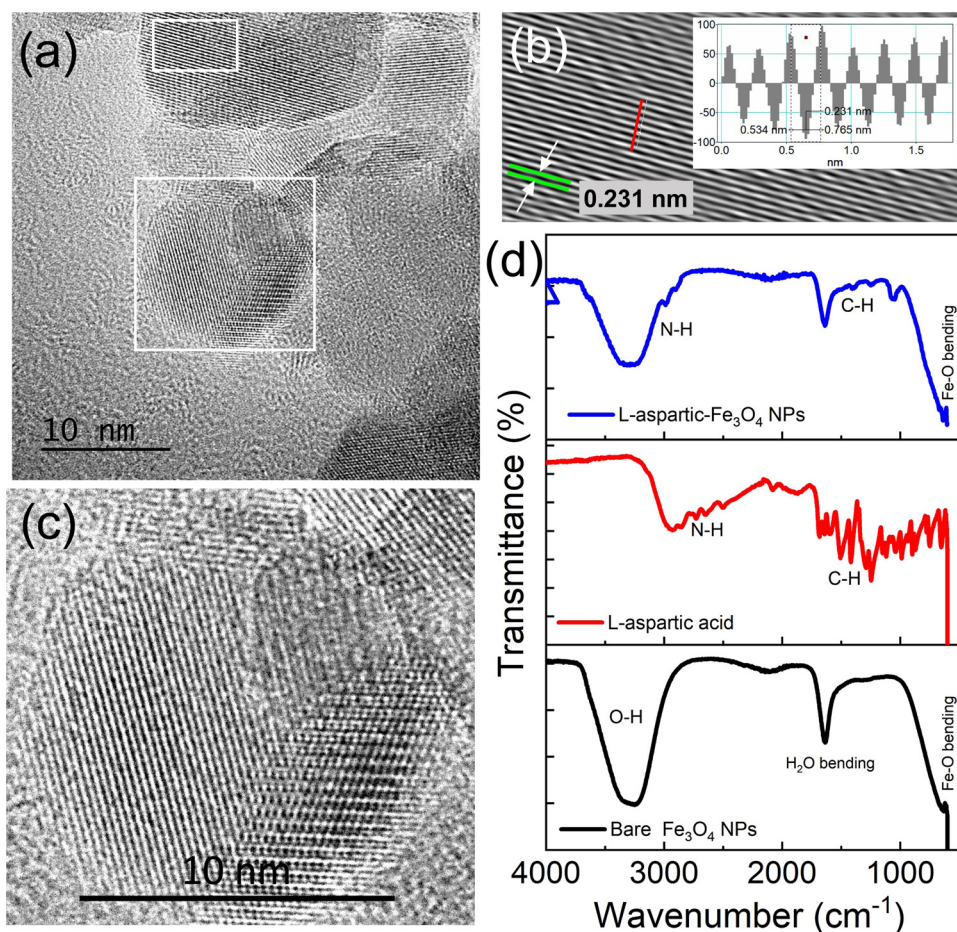
(a)
10 nm
(b)
0.231 nm
100
50
0
-50
-100
0.0
0.5
1.0
1.5
nm
0.534 nm
0.231 nm
0.765 nm
(c)
10 nm
(d)
N-H
C-H
Fe-O bending
L-aspartic-Fe_3O_4 NPs
N-H
C-H
L-aspartic acid
O-H
H_2O bending
Fe-O bending
Bare Fe_3O_4 NPs
Transmittance (%)
4000
3000
2000
1000
Wavenumber (cm^{-1})

Fig. 1. (a) High resolution TEM image of L-aspartic acid capped magnetic iron oxide (Fe_3O_4) nanoparticles (Asp-MNPs) synthesized using hydrothermal reduction process; (b) a magnified image of a section highlighted with a rectangle box in figure (a) showing calculated 0.231 nm lattice fringes and the inset figure shows surface profile showing distance of lattice fringes corresponding to the red line region; (c) A magnified section of HR-TEM image showing facetted shaped magnetic Fe_3O_4 NPs of ~12 nm size and; (d) FTIR spectra of L-aspartic acid-capped MNPs (Asp-MNPs), pure L-aspartic acid and bare MNPs.

1.25, 2.5, 5, 10, 20 ng/mL, as well as non-specific proteins including BSA, epidermal growth factor receptor-1 (EGFR1) and fibroblast growth factor (FGF) are described in SI-section.

2.8. Conjugation of MQDs with second anti-hErbB2/Her2 antibodies (Ab2)

Detailed method for functionalization of as-synthesized MQDs with second antibody (Ab2, anti-ErbB2/Her2 antibodies) that bind to the same hErbB2/Her2 target protein as Ab1 is described in SI section.

2.9. Point-of-care immuno-optomagnetic assay for detecting ErbB2/Her2 cancer biomarker

The point-of-care immuno-optomagnetic assay is designed to test serum samples with speed and accuracy, enabling physicians to take rapid and accurate diagnosis. The entire test was performed in two steps. **Step 1:** a series of spiked serum samples (100 μL each) containing 0, 0.62, 1.25, 2.5, 5, 10, 20 ng/mL of ErbB2/Her2 protein concentrations were mixed and incubated for 5 min with 10 μL of anti-hErbB2/Her2 antibody coated MQDs (MQD-Ab2). The MQDs-Ab2-hErbB2 protein complex formed was quickly pulled-down using a magnet and resuspended in 10 μL diluent (PBS, pH 7.4). **Step 2:** the entire 10 μL of MQDs-Ab2-hErbB2 protein complex from Step 1 was loaded on to respective spots-on-chip surface in duplicates that were previously immobilized with primary monoclonal hErbB2/Her2 antibodies (Ab1) and the chip was incubated for 10 min at RT. During the optimization, the chip was incubated in a petri dish dampened with a wet tissue paper that prevented from evaporation. For a negative control, 10 ng/mL BSA protein sample was added at the end of each lane on a same chip to ensure that no non-specific binding occur on chip. After the reaction, the droplet-on-chip was drained by rinsing with PBS solution and dried using a rubber bulb air blower. The signal was detected from chip after briefly flashing with a UV-torch that illuminated MQDs on chip surface and images of UV-illuminated chips were acquired using a smartphone equipped with a camera and an App (colorimeter) that computes and display RGB intensities. The intensities from fluorescence emission were analyzed by following two methods; (a) qualitative analysis of red, green and blue (RGB) ratios using a smartphone app (colorimeter app), and (b) quantitatively measuring RGB channel intensities from still images, from at least three locations per each spot-on-chip representing a specific ErbB2/Her2 concentration, and (c) fluorescence emission-on-chip and converting the fluorescence intensities into arbitrary grey values using a quantitative image processing software (ImageJ). It is to be noted that the RGB values vary among the former two different methods (a) and (b) (qualitative / quantitative), but the trend remained same, and therefore these two data-values varied. The limit of detection (LoD) concentration was estimated based on intersection of the extrapolated linear midrange and lowest concentration segment of the calibration plot. All experiments were carried out in replicates ($n = 2\sim5$) and % relative standard deviation (%RSD) was calculated to be less than 9%.

For validation, the residual sample droplet on chip after the immunoreaction was collected by gentle aspiration in a separate Eppendorf tube and the residual fluorescence intensity was measured, which is regarded as unreacted MQDs-Ab2 used to calculate the difference.

2.10. Specificity of PoC immuno-optomagnetic assay

Specificity tests of the developed immuno-optomagnetic assay was carried out using non-specific proteins (EGFR1, FGF and BSA) as described in the SI section.
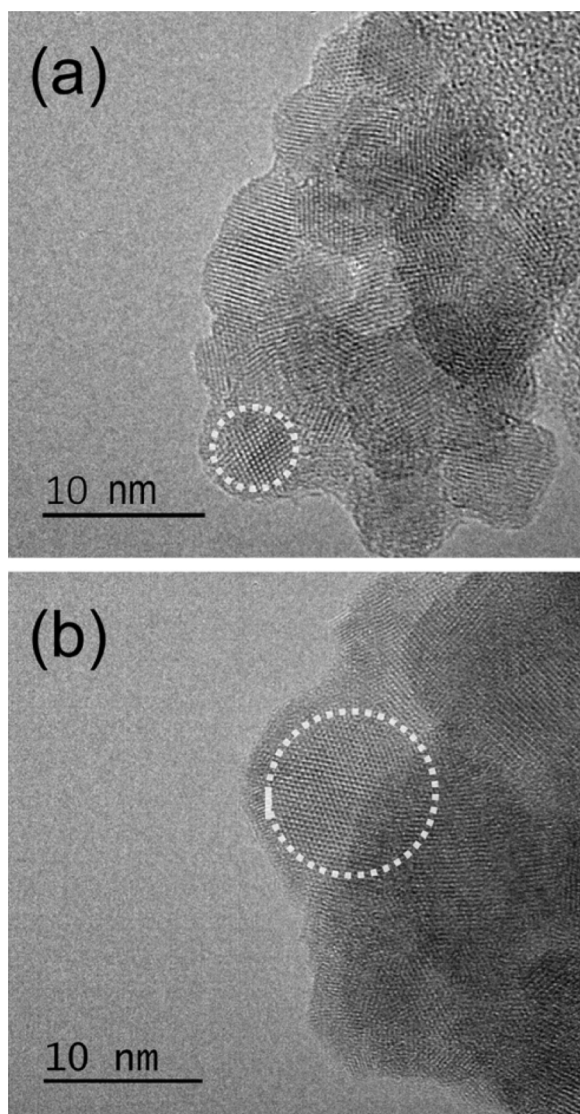
Fig. 2. High-resolution transmission electron microscopic (HR-TEM) images of CdSe/CdS/ZnS QD nanocrystals with CdSe core coated with thin gradient layers of CdS followed by ZnS (core/shell/shell). Image showing; (a) smaller ~5 nm green nanocrystals and (b) larger orange/red 10 nm nanocrystals.

3. Results and discussion

3.1. Design and synthesis of MQDs

The present study describes an immuno-optomagnetic PoC assay for rapid and sensitive detection of hErbB2 cancer biomarker in serum sample. First, magnetic quantum dots were synthesized in three stages of chemical reactions. In a first stage, Asp-MNPs were synthesized from bare-MNPs and their HR-TEM analysis revealed average size of 7~12 nm and displayed clear lattice fringes separated by 2.31 Å (Fig. 1a-c). XRD pattern of MNPs exhibited diffraction peak indices corresponding to (2 2 0), (3 1 1), (4 0 0), (1 1 0) (4 4 2), (5 1 1), (4 4 0) and (5 5 3) planes matched well with cubic spinel phase of magnetite, indicating that the synthesized MNPs has crystalline magnetite phase (Fig. S1). Fig. 1d shows FTIR spectra confirming L-Aspartic acid capping occurred on MNPs and the details on spectral analysis is described in SI-section.

In a second separate reaction, CdSe/CdS/ZnS core-shell-shell QD nanocrystals (MQDs) of two different sizes 5 and 10 nm were synthesized, and these nanocrystals were capped with polymeric dithiocarbamate chains extending free −COOH functionality by ligand

exchange process as described in experimental methods (Fig. 2a-b).

In a third stage, MQDs were synthesized by covalently coupling Asp-MNPs with two different sizes of CdSe/CdS/ZnS QD nanocrystals (5 and 10 nm). XRD-pattern of a representative MQDs sample showed corresponding indices for CdSe (100 and 220), ZnS (104 and 110) and Fe_3O_4 (200, 311, and 422) (Fig. S2a). Fig. 3a-f shows HR-TEM images and EDS maps of elements in MQDs that were identified to be Cd, Se, Zn, S, Fe and O. The EDS map showed that the QD nanocrystals were coated with aggregates of Fe_3O_4 nanoparticles forming MQDs that can be magnetically separated (Figs. 3c-f). Fig. 3g shows time-lapse images demonstrating magnetic nature of MQDs with superparamagnetic characteristics at 305 K (see SI section) by which separation of synthesized two different colored MQDs can be made in ~5 min (Fig. S2b and Supplementary video S1). The sizes of MQDs varied from 50~120 nm, which can be sorted by size fractionation. Figure S3a-e shows STEM image of another representative MQD nanoparticle and its EDX map confirming size and orientation of elemental arrangement. In this study, the QDs were designed to remain buried in the center, while they were being protected by the surface bound magnetic nanoparticles (7~12 nm sizes). This type of orientation provided following main advantages such as; (a) protection from direct exposure of central core QDs and prevented loss of QDs' emission property, (b) the fact that QDs remain buried in the center while magnetic nanoparticles form a protective shell making the MQDs architecture more biocompatible and (c) controlled MQDs sizes with respect to MNPs:QDs ratios promoting stability in optical signal and resistant to external perturbation. Such type of nano-configuration to our knowledge is not yet reported in the literature and the details are discussed in **SI section**. However, only rarely that one group [17] reported use of a different orientation MQDs, where QDs were coated on surfaces of large MNPs's that is more prone to present challenges of QDs's dissociation into solution or imminent loss of QDs' fluorescence with surround charged molecules.

These MQDs were subjected to biofunctionalization with monoclonal anti-hErbB2 antibodies (Ab2), which gave rise to a multimodal MQDs-Ab2 as described in experimental methods. The MQDs-Ab2 in this study provided multimodal functionality that comprised of; (a) biorecognition and capturing of biomarker from serum, (b) magnetic separation to concentrate or isolation of target biomarker from bulk and dilute serum sample, and (c) easy and visible detection of immunooptomagnetic signal upon its binding with the analyte, more specifically MQDs-Ab2-analyte complex that was employed for PoC detection. Moreover, MQDs were fabricated with unique architecture designed to display nano-scale orientation in which core QD nanocrystals were shielded by surrounding layers of MNPs and preserved emission efficiency, prevents photobleaching and display stable fluorescence emission upon illumination with a simple UV-troch and biocompatible. Taken together, these MQDs were applied for developing an immunooptomagnetic PoC diagnosis assay, specifically for detection of a model hErbB2 protein in serum.

3.2. Point-of-care (PoC) immuno-optomagnetic assay

The PoC immuno-optomagnetic assay was performed using a fabricated PoC chip platform as illustrated in Scheme 1a-f and described in experimental methods. First, silane activated borosilicate chips were functionalized with anti-hErbB2 antibodies (Ab1) in arrays of 5 mm diameter, each separated by a distance of 5 mm. The immuno-optomagnetic assay chip carried 8-pairs of immunoreaction spots, sufficient to detect six pairs of varying biomarker concentrations in duplicates and a pair of spots each for negative control/blank. This chip was tested for its applicability in sensing a breast cancer disease biomarker as a model analyte, which currently possible only using ELISA [8,9], FISH [5–7] or undergo mammogram, tissue biopsy, CT, MRI, CAT or PET scans [2,3] that all require functional laboratory or hospitals. The assay designed in this study does not require any such facility to conduct assay as compared with those reported previously and the details are
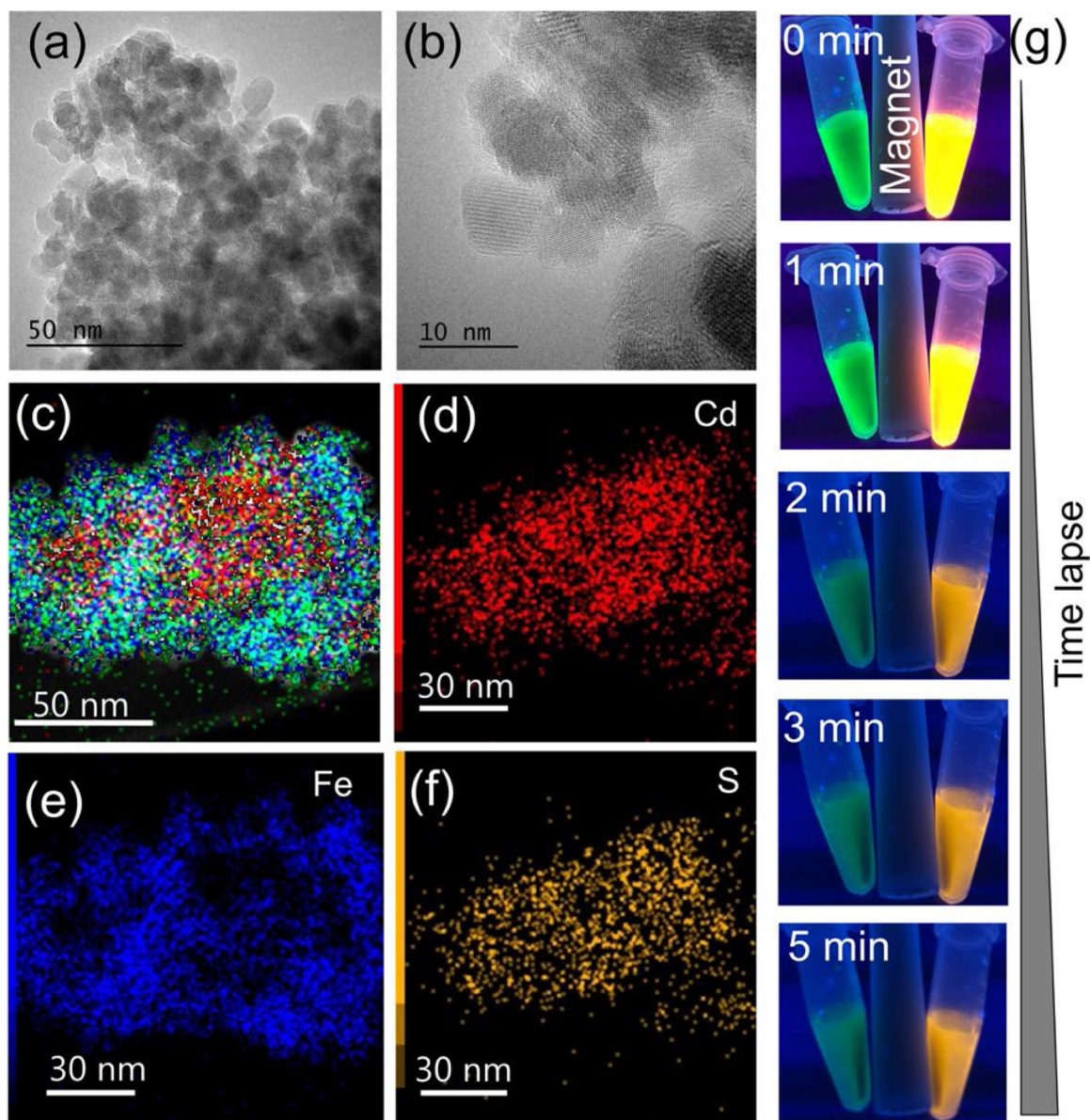
Fig. 3. (a and b) HR-TEM images of MQDs at different magnifications. (c) An overlaid EDS map of MQDs showing different colors representing different elements of MQDs. (d-f) Individual maps for Cd, Fe and S elements, respectively derived from MQDs. The red and orange colors representing Cd and S elements, respectively were found surrounded by Fe elements forming MQDs. (g) Time-lapse images taken during the magnetic separation process using a magnet from $0 \sim 5$ min with two different colloidal magnetic quantum dots (MQDs) with emissions at 525 nm and 585 nm, respectively. Magnetic separation of MQDs can be observed in Supplementary video S1.

discussed in **SI-section**. For this, a series of hErbB2 protein spiked serum samples were prepared in hErbB2-free serum as described in experimental methods. Spiked serum samples containing varying concentrations of hErbB2 protein ($0 \sim 20$ ng mL^{-1}) were allowed to interact with MQD-Ab2 by simple mixing for 10 min and magnetic separation followed by dispersion in a small volume of diluent (10 µL PBS). Here, MQDs-Ab2 were previously bioconjugated with a second type of anti-hErbB2 antibodies distinct from Ab1 ensuring its binding to distinct epitopes of a same analyte. MQDs-Ab2 allowed specific capturing of serum hErbB2 protein giving rise to a complex of MQDs-Ab2 and hErbB2 protein (MQD-Ab2-hErbB2) (Scheme 1b–d).

The magnetic nature of MQD-Ab2-hErbB2 complex allowed rapid separation by bringing close to an external magnetic field tracking its fluorescence emission. Therefore, entire MQD-Ab2-hErbB2 complex formed was purified/isolated and concentrated from serum, which was later charged on to PoC immuno-optomagnetic chip pre-activated with Ab1 for specific detection. After chip incubation for 10 min at 37 °C, the

unreacted/free MQD-Ab2 on chip was removed and the residual fluorescence levels was measured for stoichiometric comparison. Signal from the chip was visually inspected while flashing the chip with a simple hand-held UV-torch that illuminated MQD-Ab2-hErbB2 complex formed on chip. The intensity of fluorescence emission from MQD-Ab2-hErbB2 complex-on-chip was directly proportional to target analyte concentration, which provided the levels of hErbB2 cancer biomarker present in the test serum samples. Fig. 4a shows signal generated from the PoC immuno-optomagnetic assay chip, which was recorded using still 8-bit RGB images from replicate chips for accurate quantitative estimations, while Fig. 4b–g show the data derived from a simple smartphone camera and a colorimeter app equipped with image processing and RGB-computing algorithm in android operating system (qualitative data). The app computed the red, green and blue (RGB) channel intensities from UV-excited MQDs' fluorescence emission signal on chip, which was used for rapid qualitative detection of the biomarker concentrations with reference to standard controls. However, it
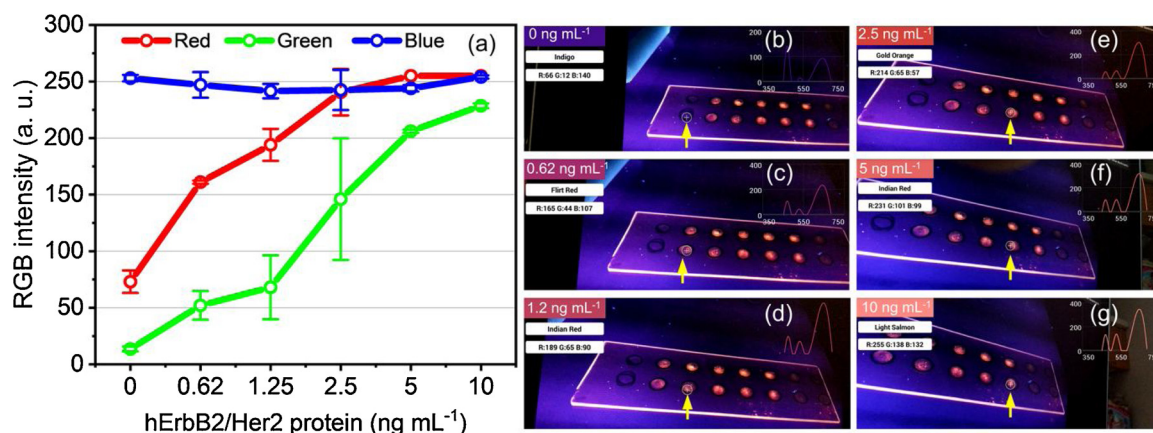
Fig. 4. (a) Red, green and blue (RGB) intensities against varying hErbB2 protein. The data is derived from quantitative analysis of 8-bit RGB still images of UV-illuminated chips taken by a smartphone camera equipped with RGB-computing algorithm in an android operating system. The algorithm computed RGB intensities in replicate measurements ($n = 2$ to 5) corresponding to varying cancer biomarker concentrations ($0 \sim 10$ ng mL^{-1} serum hErbB2/Her2 protein) form chip. Figures (b-g) shows screenshot images (qualitative data) of a smartphone during the rough alignment of cursor/pointer on each spot-on-chip (highlighted manually by arrows) that displayed respective RGB values in relation to a specific biomarker concentration present in the test serum sample, respectively (shown in the insets). The insets in (b-g) also show a spectra of intensities against the function of wavelengths which is a part of display output in smartphone app (colorimeter). The RGB values on the top left corners in (b-g) are highly dynamic and subject to variation and therefore different from those shown in plot (a).
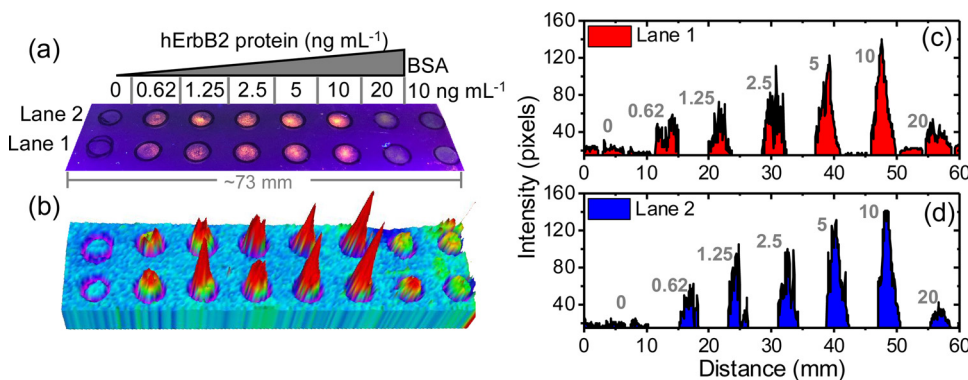

Fig. 5. (a) Real image of point-of-care (PoC) immunoassay chip exposed to UV light (365 nm) taken by a smartphone camera showing fluorescence emission from MQD-Ab2-hErbB2 complex that was captured by Ab1 present on chip. The concentration dependent increase in fluorescence intensity corresponded to the increasing levels of hErbB2 in serum until saturation level at 10 ng mL^{-1}. (b and c) 3D profile and area under the plot map generated using fluorescence intensities from Lanes 1 and 2 from image (a), respectively were calculated as intensity (pixels) using image processing software (ImageJ) and plotted as a function of mm distance on chip.

is to be noted that the RGB values in Fig. 4a and b–g cannot be compared as they were derived from two different methods as described in experimental section. RGB values in Fig. 4b–g were highly dynamic and therefore they represented for only qualitative analysis. This was largely because of the highly dynamic and variable RGB-values displayed real-time on smartphone screen (screenshot images in Fig. 4b–g), which is more prone to dynamic changes in intensities with even slightest movement of cursor/pointer as opposed to still images and therefore, different from those in Fig. 4a. The algorithm computed RGB intensity values corresponding to varying cancer biomarker concentrations tested ($0 \sim 20$ ng mL^{-1} serum hErbB2/Her2) using PoC chip. The 8-bit ($2^8 = 256$) different RGB levels provided greater precision and computed small changes in colors especially originating from the fluorescence emission by MQDs-on-chip, which was directly proportional to the cancer biomarker levels in test serum sample.

Detection of serum hErbB2 protein was made within $15-30$ min of sample loading that required no additional steps or reagents. Fig. 4(b–g) shows representative screenshot images of a smartphone application after cursor/pointer alignment on each spot-on-chip (highlighted by arrows) that displayed respective RGB values proportional to specific biomarker concentrations present in the test serum sample. The color variants with respect to biomarker levels shown embedded in respective images as a part of smartphone application display output (Fig. 4b–g insets). Only red (R) and (G) channels were responsive to MQDs, while G channel had more accuracy than R that displayed concentration dependent increasing intensity values until reaching to a saturation point at 10 ng mL^{-1} of hErbB2/Her2 protein

against the blue (B) background (Fig. S4a). The blue (B) channel however, remained unaffected during the entire immunoassay process and therefore its response served as a background noise control. The linearity and detection ranges was extrapolated from the data that exhibited wide linear range from 620 picograms mL^{-1} to 5 nanogram mL^{-1} (Fig. S4a) which is well within the acceptable clinical range [6,8,11].

PoC immuno-optomagnetic assay chip response was validated using a conventional image processing using ImageJ software that exhibited a dynamic detection range from $0.62 \sim 10$ ng mL^{-1} hErbB2/Her2 biomarker protein in serum with LoD of 165 pg/mL hErbB2/Her2 with green channel and 942 pg/mL with red channel. This optical signal was although distinguishable by visual inspection of chip from 625 pg mL^{-1} to 5 ng mL^{-1} hErbB protein simply while flashing UV-torch, which is consistent with the extrapolated LoD range (Fig. S4a). However, distinguishing chip-signal from any levels beyond LoD range required sensitive measurements be made either by fluorescence emission spectra or calculating pixel density using image processing software. Fig. 5a shows an image of UV-illuminated PoC immunoassay chip captured post-immunoreaction by a smartphone camera. The fluorescence emissions from MQD-Ab2-hErbB2 complex and their signal intensities proportional to varying hErbB2 biomarker levels were calculated based on pixel intensities. This result demonstrated that the broader dynamic range of diagnostic signal from developed PoC immunoassay chip can also be accurately measured by conventional methods to distinguish concentration-dependent linear increase in fluorescence intensities (Fig. 5a,b). Quantified pixel intensities from the

UV-exposed chips was consistent to visible inspection made, as well as that by using a simple smartphone camera and a colorimeter app (Figs. 5c,d; 4 a–g). Visible detection however is more suitable for PoC applications especially at resource limited settings as a qualitative result, but the trend remains comparable to quantitative estimation (Figs. 4a and 5 c.d).

Specificity of MQDs was governed by the embedded hErbB2/Her2 specific monoclonal antibodies (Ab2) that self-fractionated-on-chip following binding on to a second hErbB2/Her2 antibody (Ab1) tethered on chip making it more conveniently separate free or unreacted MQDs-Ab2. The residual un-reacted MQD-Ab2 was therefore collected post-reaction from the chips and measured residual fluorescence intensities to calculate the stoichiometric concentrations of unbound-MQD-Ab2 and MQD-Ab2-hErbB2. Figure S3b shows fluorescence spectra of un-reacted MQD-Ab2 exhibited decreasing residual fluorescence intensity levels that corresponded well with increasing fluorescence intensities observed with MQD-Ab2-hErbB2 complex-on-chip, and this trend was directly proportional to the levels of target hErbB2 protein present in the test serum sample. It is to be cautioned that the residual MQDs-Ab2 cannot be accounted for accurate estimation due to the loss of some fraction while withdrawing from the chip-surface. However, this could be considered for establishing relationship of dose-dependency by comparison with response of immuno-optomagnetic assay.

3.3. PoC specificity

Specificity tests of the developed PoC immuno-optomagnetic assay was carried out under identical conditions as described in experimental section for hErbB2 detection. Three different samples, such as (a) blind serum samples containing target hErbB2 protein were used as positive controls, (b) serum sample spiked with three different concentrations of three different non-specific proteins (negative controls), such as epidermal growth factor receptor-1 (EGFR1, a structurally similar protein to human ErbB2) in triplicates of 5 and 2.5 ng mL^{-1}, FGF, which is a co-existing protein in serum (1, 5 and 10 ng mL^{-1}) and (c) bovine serum albumin (BSA) protein spiked serum as a second negative control. Figure S5a-b show results of specificity tests carried out using PoC immuno-optomagnetic assay chip under standard assay conditions similar to that described for detection of hErbB2. Specificity tests revealed successful detection of hErbB2 protein in blind serum sample corresponding to 2.5 and 5 ng mL^{-1} that matched to the expected levels. It is evident from Fig. S5a-b that the PoC immunoassay did not show cross reactivity with non-specific proteins, such as one that is structurally similar ErbB1 (EGFR) protein or FGF or BSA proteins, indicating that the PoC immuno-optmagnetic assay reaction presented high specificity to hErbB2 protein in serum with a detection range from 0.62 to 5 ng mL^{-1} hErbB2/Her2 under standard assay conditions using a smartphone. This detection range can be more accurately extended up to 10 ng mL^{-1} provided that a conventional image processing (ImageJ) tool is required to analyze data for the accurate signal measurements.

4. Conclusions

In this study, a novel immuno-optomagnetic PoC chip assay is developed which utilizes multifunctional MQD nanocrystals on bioactivated PoC-chip for detection of hErbB2 cancer biomarker protein in human serum. The assay relies on use of bioactivated MQD-nanoarchitectures as nanoprobes that were uniquely designed for simultaneously exhibiting both magnetic and optical properties for capturing of target biomarker in serum. These MQDs were non-dissociable because of their orientation, where CdSe/CdS/ZnS QD nanocrystals forms the central core material shielded by a coating of thick layer of MNPs. QD nanocrystals in MQDs remain inaccessible to external environment and therefore prevented from quenching or loss of optical properties. The signal detection is made simply by flashing the chip with a hand-held UV-torch and a smartphone equipped with camera and RGB processing application. Detection of serum hErbB2 protein is made within 30 min of sampling that required no additional steps, equipment or reagents, which was sufficient to detect well below the clinically normal levels (625 pg mL^{-1} to 5 ng mL^{-1}). We envision that this immuno-opto-magnetic PoC chip assay can be extended to detecting various other disease biomarkers and potentially be used in a resource limited settings.

CRediT authorship contribution statement

Anjum Qureshi: Conceptual design of experiments, conducted experiments – MQDs synthesis, physicochemical characterizations, assay validation, writing – review & editing the manuscript.

Ali Tufani: Chemical synthesis of QDs, post-synthesis modifications, physicochemical characterizations and validation.

Gulcan Corapcioglu: High-resolution and Scanning TEM analysis, elemental map of QDs/MQDs

Javed H. Niazi: Conceptualization, conducting PoC detection experiments and validation, writing – review & editing, project administration, supervision, funding acquisition.

All authors have given approval to the final version of the manuscript.

Declaration of Competing Interest

The authors declare that they have no known competing financial interests or personal relationships that could have appeared to influence the work reported in this paper.

Acknowledgments

Appendix A. Supplementary data

Supplementary data associated with this article can be found, in the online version, at doi:https://doi.org/10.1016/j.snb.2020.128431.

References

[1] WHO, W.h.o. WHO, 2018, https://www.who.int/cancer/prevention/diagnosis-screening/breast-cancer/en/.

[2] M. Grapin, C. Coutant, J.M. Riedinger, S. Ladoire, F. Brunotte, A. Cochet, O. Humbert, Eur. J. Radiol. 113 (2019) 81–88.

[3] T. Ha, Y. Jung, J.Y. Kim, S.Y. Park, D.K. Kang, T.H. Kim, Clin. Radiol. 74 (10) (2019) 817 e815–817 e821.

[4] C. Forbes, D. Fayter, S. de Kock, R.G. Quek, Cancer Manag. Res. 11 (2019) 2321–2337.

[5] M.H. Lee, S.-Y. Jung, S.H. Kang, E.J. Song, I.H. Park, S.-Y. Kong, Y.M. Kwon, K.S. Lee, H.-S. Kang, E.S. Lee, PLoS One 11 (10) (2016) e0163370-e0163370.

[6] T. Sasaki, N. Fuse, T. Kuwata, S. Nomura, K. Kaneko, T. Doi, T. Yoshino, H. Asano, A. Ochiai, Y. Komatsu, N. Sakamoto, A. Ohtsu, Jap. J. Clin. Oncol. 45 (1) (2014) 43–48.

[7] J. Veeraraghavan, C.D. Angelis, R. Mao, T. Wang, S. Herrera, A.C. Pavlick, A. Contreras, P. Nuciforo, I.A. Mayer, A. Forero, R. Nanda, M.P. Goetz, J.C. Chang, A.C. Wolff, I.E. Krop, S.A.W. Fuqua, A. Prat, S.G. Hilsenbeck, B. Weigelt, J.S. Reis-Filho, C. Gutierrez, C.K. Osborne, M.F. Rimawi, R. Schiff, Ann. Oncol. 30 (6) (2019) 927–933.

[8] T. Fehm, S. Becker, S. Duerr-Stoerzer, K. Sotlar, V. Mueller, D. Wallwiener, N. Lane, E. Solomayer, J. Uhr, Breast Cancer Res. 9 (5) (2007) R74.

[9] J. Tchou, L. Lam, Y.R. Li, C. Edwards, B. Ky, H. Zhang, Springer Plus. 4 (1) (2015) 237.

[10] P. Bhusari, R. Vatsa, G. Singh, M. Parmar, A. Bal, D.K. Dhawan, B.R. Mittal, J. Shukla, Int. J. Cancer 140 (4) (2017) 938–947.

[11] A.S.C. Fabricio, S. Michilin, M. Zancan, V. Agnolon, L. Peloso, R. Dittadi, A. Scapinello, C. Ceccarelli, M. Gion, Scand. J. Clin. Lab. Invest. 79 (4) (2019) 260–267.

[12] S.-W. Luoh, W. Wagoner, X. Wang, Z. Hu, X. Lai, K. Chin, R. Sears, E. Ramsey, Mol. Carcinog. 58 (5) (2019) 699–707.

[13] N. Iqbal, N. Iqbal, Mol. Biol. Int. 2014 (2014) 852748-852748.

[14] D.P. English, D.M. Roque, A.D. Santin, Mol. Diag. Ther. 17 (2) (2013) 85–99.
[15] Q. Ma, Y. Nakane, Y. Mori, M. Hasegawa, Y. Yoshioka, T.M. Watanabe, K. Gonda, N. Ohuchi, T. Jin, Biomaterials 33 (33) (2012) 8486–8494.
[16] K.D. Mahajan, Q. Fan, J. Dorcéna, G. Ruan, J.O. Winter, Biotechnol. J. 8 (12) (2013) 1424–1434.
[17] Z. Rong, Z. Bai, J. Li, H. Tang, T. Shen, Q. Wang, C. Wang, R. Xiao, S. Wang, Biosens. Bioelectron. 145 (2019) 111719.
[18] C. Kim, P.C. Searson, Nanoscale 7 (42) (2015) 17820–17826.
[19] K.D. Mahajan, G.B. Vieira, G. Ruan, B.L. Miller, M.B. Lustberg, J.J. Chalmers, R. Sooryakumar, J.O. Winter, Chem. Eng. Prog. 108 (2012) 41.
[20] G. Ruan, G. Vieira, T. Henighan, A. Chen, D. Thakur, R. Sooryakumar, J.O. Winter, Nano Lett. 10 (6) (2010) 2220–2224.
[21] C. Tuerk, L. Gold, Science 249 (4968) (1990) 505–510.
[22] V. Panwar, P. Kumar, A. Bansal, S.S. Ray, S.L. Jain, Appl. Catal. A Gen. 498 (2015) 25–31.
[23] W.K. Bae, K. Char, H. Hur, S. Lee, Chem. Mat. 20 (2) (2008) 531–539.
[24] Y. Wang, V.D. Ta, Y. Gao, T.C. He, R. Chen, E. Mutlugun, H.V. Demir, H.D. Sun, Adv Mater. 26 (18) (2014) 2954–2961.

Dr. Anjum Qureshi received her Ph.D. degree in Physics in 2008 from MS University of Baroda, India. She is currently working as a research faculty at Sabanci University Nanotechnology Research & Application Center, Turkey. Her research interests include studying physics of biological systems, detection of diseases biomarkers by electro-chemical biosensors and modification of polymer nano-composites for designing new bio-/chemical sensors. She received several national grants as a PI and successfully completed all of them and her current research is focused on wearable biosensors.

Dr. Ali Tufani received his Ph.D. degree in Materials Science and Nano Engineering from Sabanci University in 2018. During his Ph.D. program, he worked on initiated Chemical Vapor Deposition (iCVD) for different applications like nanotubes and electrospun fibers for drug delivery and membranes for proteins and macromolecules separation. Recently, he works in Dr. Javed's Biosensor and Biomolecular Technology Lab as the postdoctoral fellow.

Dr. Gulcan Corapcioglu received her Ph.D. in Materials Science and Nano Engineering from Sabanci University in 2016. Currently is working as a Researcher in the field of nanomaterials for photonics applications and atomic level characterization of nanos-tructures at Sabanci University Nanotechnology Research and Application Center (SUNUM).

Dr. Javed H. Niazi received his Ph.D. degree in Biochemistry in 2003 from Gulbarga University and worked as a visiting scientist and Research Professor from 2004 to 2009 in Rep. of Korea (GIST, KIST and Korea University) to work on design and development of recombinant bacterial biosensors. He moved to Sabanci University in 2009 as a visiting faculty and since 2011, he is working as a research faculty in Sabanci University Nanotechnology Research & Application Center (SUNUM), Istanbul. His work spans from cellular and molecular engineering and electrochemistry to bio-inspired synthetic bio-/nano-materials that are targeted toward designing analytical reagents and biosensors with recognition and signal transduction capabilities and received grants as a PI of several research projects.